# Photoelectrocatalytic Removal of Color from Water Using $TiO_2$ and $TiO_2/Cu_2O$ Thin Film Electrodes Under Low Light Intensity

**Z. Feleke, R. van de Krol, and P.W. Appel**

**Abstract** This work describes, photoelectrocatalytic degradation of organic pollutants by using methyl orange (an azo dye) as a model compound. The $TiO_2$ thin film and $TiO_2/Cu_2O$ composite electrodes were used as semiconductor photo electrodes. Photo catalysis by UV light Corresponding to the light intensity range of the solar light was employed with the aim of using renewable and pollution-free energy. Result showed that the rate of removal of color was enhanced when potential bias of 1.5 V was applied. The degradation rate was also increased either in acidic (pH 2) or alkaline (pH 10) conditions. The application of a positive potential higher than the flat-band potential on the $TiO_2$ electrode decreases the rapid charge recombination process, and enhanced the degradation of organic compound. When the $TiO_2/Cu_2O$ thin film electrode was used, more efficient electron and hole separation was observed in the composite system under very low potential. It is considered that the photo-generated holes migrate towards the interface while the electrons migrate towards $TiO_2$ and then to the back contact transparent fluorine doped tin-oxide-coated glass (TCO), making the behavior of the composite film analogous to that of an n-type semiconductor. In all cases, the kinetics of the photo catalytic oxidation of methyl orange followed a pseudo first order model and the apparent rate constant may depend on several factors such as, the nature and concentration of the organic compound, radiant flux, the solution pH and the presence of other organic substances.

**Keywords** Photoelectrocatalysis · titanium dioxide · cuprous oxide · composite thin film · photo electrode

---

Z. Feleke (✉)
Department of Chemistry, Faculty of Science, Addis Ababa University, P.O. Box 1176,
Addis Ababa, Ethiopia
e-mail: *zewge@chem.aau.edu.et* or *fbeshah@yahoo.com*

R. van de Krol and P.W. Appel
Department of Chemical Technology, Faculty of Applied Science, Delft University
of Technology, Julianalaan 136, 2628 BL Delft, The Netherlands

E.K. Yanful (ed.), *Appropriate Technologies for Environmental Protection in the Developing World*,

# 1 Introduction

Photo catalytic processes to degrade organic pollutants in water by oxidation utilizing $TiO_2$ as a catalyst in the form of suspended $TiO_2$ powder have been the subjects of extensive research recently [1–4]. In practice, the rapid unfavourable electron-hole recombination reaction in $TiO_2$ compared with the relatively slow redox reactions of organic compounds resulted in low quantum yield [5, 6].

Modifications of semiconductor surfaces such as addition of metals as dopant or combinations with other semiconductors have been considered to decrease the electron and hole recombination rate and thereby increase the quantum yield of photocatalytic process [7–9]. Coupling of two semiconductor particles with different band gap energy levels has also been considered either to minimize electron-hole recombination or to modify the catalyst so as to absorb light from the sun in the visible region. A variety of semiconductor heterojunctions such as $CdS/TiO_2$, CdS/PbS, CdS/ZnO, CdS/AgI, $Cd_3P_2/TiO_2$ and $Cd_3P_2/ZnO$ and $AgI/Ag_2S$ have been investigated [10–16]. Further improvements have been reported by employing photoelectrochemical approach [17]. However, most of the semiconductor materials with relatively shorter band gap have very low stability for the purpose of water purification.

Among the numerous transition metal semiconducting oxides, cuprous oxide ($Cu_2O$) is of intense interests and has been extensively investigated for its distinctive properties. $Cu_2O$ is a reddish p-type semiconductor with a direct band gap of 2.0–2.2 eV [18, 19]. $Cu_2O$ has been tested as photo electrode in electrochemical cells and water-splitting materials [20–21], investigated the photocatalytic degradation of cyanide in water using titanium dioxide/copper oxide composite catalyst system in powder form. Vigil et al. [22] Studied the incorporation of copper oxide to nanoporous $TiO_2$ from an aqueous solution of copper formate with the purpose of sensitizing the $TiO_2$ to wavelengths in the visible range for the application of heterojunctions in solar energy. Based on the direction and wavelength dependence of photocurrent they show that photons are absorbed by the copper oxide and electrons injected to the $TiO_2$. Most of the studies reported in the literature use high intensity UV lamp, which makes it difficult for wide applications.

In the present work, photoelectrocatalytic approach was considered using both $TiO_2$ thin film electrode and $TiO_2/Cu_2O$ composite electrode. The objectives of the study were to investigate the photoelectrocatalytic activity of titanium dioxide ($TiO_2$) thin film, and electrodes titanium oxide ($TiO_2$)/cuprous oxide ($Cu_2O$)/ composite thin film electrode for the destruction of organic contaminants in water under low light intensity by using methyl orange as a model organic compound. We have focused our attention on the low-intensity range of UV illumination, from 1 to 2 mW/cm in our studies, since the ultraviolet light in direct sunlight is generally 2–4 mW/cm depending on the geographical location.

# 2 Experimental

## 2.1 Preparation of $Cu_2O$ Thin Film

$Cu_2O$ was electrodeposited on a transparent conducting substrate TCO, from alkaline Cu (II) lactate aqueous solution [23, 24] in a conventional two-electrode cell. Prior to electrodeposition, the TCO was sonicated in ethanol solution and dried in air. Copper wire was glued to the conducting side using aqueous based graphite conductive adhesive. The pH of the solution was adjusted between 9 and 12 by the addition of sodium hydroxide. The solution temperature was kept constant during deposition by a thermostat (IKA. ETS-D4 fuzzy, The Netherlands). Deposition temperature was varied in the range from 25 °C to 60 °C. The deposition potential was maintained at −0.4 V and the current density varied from 0.1 to 0.8 mA/cm$^2$. The duration of deposition ranging from 2 to 30 min was used to obtain films of various thickness. All potentials are reported versus the SCE reference electrode. Electrochemical deposition was controlled by an EG&G 283 potentiostat. Cuprous oxide films were annealed in air at 300 °C for 1 h or used without annealing. The structure of the films was identified by X-ray diffraction (XRD) under $\theta$–$2\theta$ mode (AXS D8 Advance, Bruker, England).

## 2.2 Preparation of $TiO_2$ and $TiO_2/Cu_2O$ Composite Thin Film Electrodes

$TiO_2$ films were prepared from pure Anatase Paste (ECN, The Netherlands). Two types of paste were used to prepare the $TiO_2$ electrode with different particle size 9 and 100 nm. The electrodes are represented as E1 (9 nm) and E2 (100 nm). Then, the films were annealed in air at 450 °C for 3 h in a furnace equipped with temperature control unit. The $TiO_2/Cu_2O$ composite film was prepared by electrodepositing the $Cu_2O$ on to the $TiO_2$ film from alkaline copper lactate solution at bath temperature of 60 °C. To vary the amount of deposited $Cu_2O$, the time of deposition was varied from 2 to 30 min.

## 2.3 Measurement of Photoelectrochemical Response

The photoelectrochemical measurements were performed in a single compartment Teflon cell having 1 cm diameter circular quartz three-electrode system. The light source was a light emitting diode (LED) with maximum emission of 375 nm (FWHM~15 nm, Roithner) array that was aligned for proper sample illumination. The potential was controlled with the potentiostat (EG&G 283, The Netherlands).

Current–time and current-voltage measurements were made in 0.5 M $K_2SO_4$ solution. For quantitative photoelectrochemical characterization at different wavelength, white light from a halogen lamp (200 W, Osram, The Netherlands) in an Oriel housing was passed through a monochromator (Spectropro150, Acton). The light intensity was measured with a UV photodiode (PD300, Ophir, Germany). The spectral photo response was measured with a potentiostat (EG&G 283, The Netherlands) equipped with shutter (UNIBLITZ, Model T132, France). The photo response was measured with and without oxygen bubbling.

## 2.4 Photo catalysis and Photoelectrocatalysis Experiments

The photocatalytic activity of the $TiO_2$ thin film electrodes and the $Cu_2O/TiO_2$ composite thin film electrode was evaluated using -[4-(dimethylamino)phenylazo] benzenesulfonic acid (methyl orange) as a model compound (Fig. 1). Screening photo catalysis experiments were carried out using rectangular 3 mL capacity quartz cell. The light source was a deuterium lamp with light intensity of 2 mW/cm$^2$ (Model C4545, Germany). Further photocatalytic (PC) and photoelectrocatalytic (PEC) degradation experiments were performed in a single-compartment Teflon cell (40 mL) reactor having a circular quartz window of 20-mm diameter (Fig. 2). A circular opening in the cell opposite to the quartz window allowed exposure of 3.14 cm$^2$ of the working electrode ($TiO_2$ or $TiO_2/Cu_2O$) to UV illumination. The platinum coil counter electrode was placed just in front of the working electrode. A saturated calomel electrode (SCE), used as a reference, was placed close to the working electrode. The experiments were carried out in the pH range from 2 to 10 in 0.1 M $K_2SO_4$ or 0.1 KCl

**Fig. 1** [4-(Dimethylamino)phenylazo]benzenesulfonic acid, sodium salt (methyl orange)

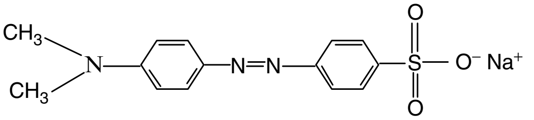

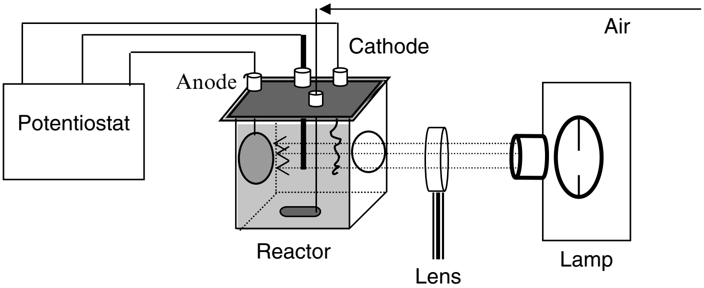

**Fig. 2** Schematic diagram of photocatalysis and photelectrocatalysis reactor system

M electrolyte solutions. A potentiostat model EG&G 243 was used to bias the working electrode. Unless noted otherwise, the concentration of dyes used was 20 mg/L. Aqueous solution of methyl orange (40 mL) was photolysed under various operating conditions. The pH of the solution was adjusted to desired value with sodium hydroxide and sulfuric acid solution. The potential was controlled with the potentiostat (EG&G 243). The photo degradation of methyl orange was monitored with UV-Vis spectrophotometer (VARIAN) at its wavelength of maximum absorption (464 nm).

# 3 Results and Discussion

## 3.1 Film Compositions and Structure

The XRD spectrum of film sample, deposited on tin oxide conducting glass (TCO) substrate from lactate solution under alkaline medium is shown in Fig. 3. The film deposited is polycrystalline and chemically pure $Cu_2O$ with no traces of CuO. The XRD spectrum indicates a strong $Cu_2O$ peak with (200) preferential orientation. This is in good agreement with the results of other studies [23, 25, 26].

## 3.2 Photo Response

The dark and photocurrent of the $Cu_2O$ electrode at -0.4 V vs. Ag/AgCl is represented in Fig. 4. A typical p-type photocurrent versus time behavior is observed. In

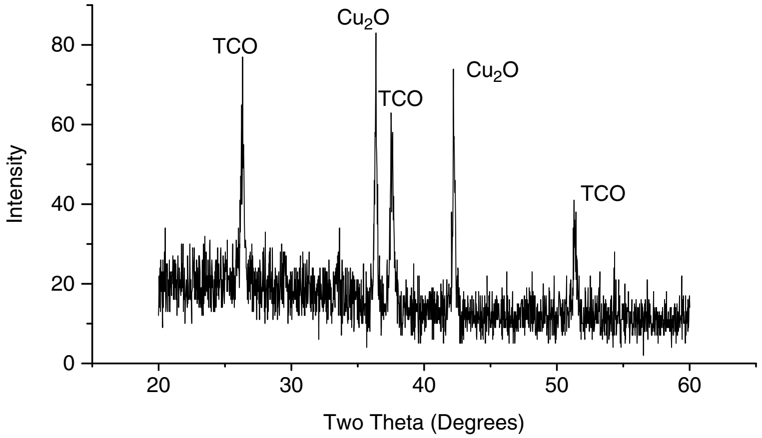

**Fig. 3** X-ray diffraction patterns of copper oxides deposited at −0.4 V on TCO from alkaline lactate solution pH 10

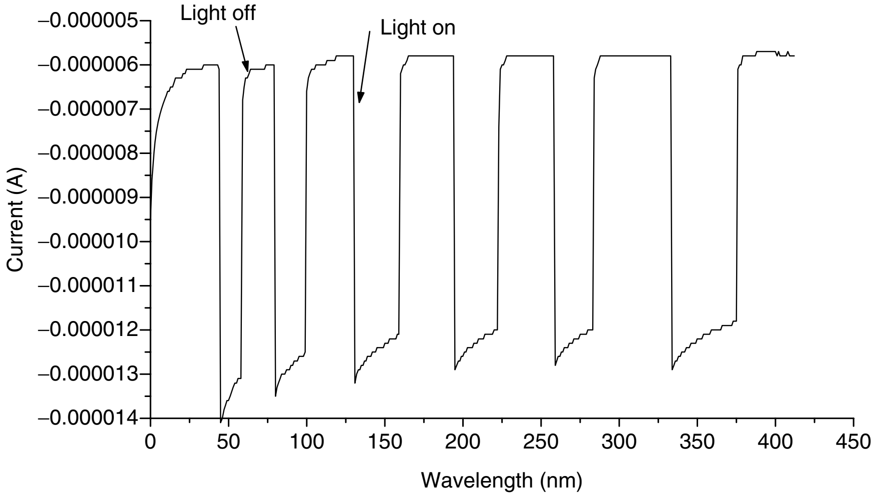

**Fig. 4** Photo response $Cu_2O$ electrodeposited from alkaline lactate solution on TCO conduction substrate under oxygen bubbling (0.5 M $K_2SO_4$, 0.2 mA/cm$^2$, –0.4 V)

addition, Photocurrent was stable over longer time range. The photo response was not changed after repeated use of the electrode and similar photo response was obtained for films deposited for 2, 5, 10, 20, and 30 min (data not shown). This indicates that the overall process of light absorption by the semiconductor, generation and separation of electron hole pairs, and transfer of electrons, is efficient even for thick films.

The cyclic voltammogram of the $Cu_2O$ thin film electrode in 0.5 M $K_2SO_4$ solution in the dark and under illumination (375 nm) is shown in Fig. 5. The sweep starts at open-circuit potential and is scanned cathodically at 10 mV/s. At potential more negative than −0.8 V vs. SCE, a fast increasing cathodic current was observed due to the reduction of $Cu_2O$ to Cu, which is also reported by other researchers [24]. The deposition currents are in a potential window between –0.3 and –0.7 V, which is about 400 mV window. The potential range corresponds to the Pourbaix diagram for the stability of Cu, $Cu_2O$, and CuO system [27]. Other studies on the electrochemical deposition of $Cu_2O$ oxide films showed that the potential window is between –0.35 and –0.55 V [23]. The deposition current in Fig. 5 is very stable indicating that the p-type electrode containing $Cu_2O$ as main component is resistant against photo corrosion. Figure 6 shows the spectral photo response of the electrodes prepared from alkaline lactate solution at pH 10. The photoresonse region of $Cu_2O$ lies in the UV and visible region (300–600 nm) with absorption maximum around 450 nm. The maximum instantaneous photocurrent efficiency (IPCE) calculated from Equation (1) at 375 nm is 7%. This value is comparable to the value reported by Jongh et al. [24] for absorption in the visible region, but lower for absorption in the UV region. The photocurrent measurement in this study was carried out without air bubbling. The spectral photo response of the $TiO_2/Cu_2O$

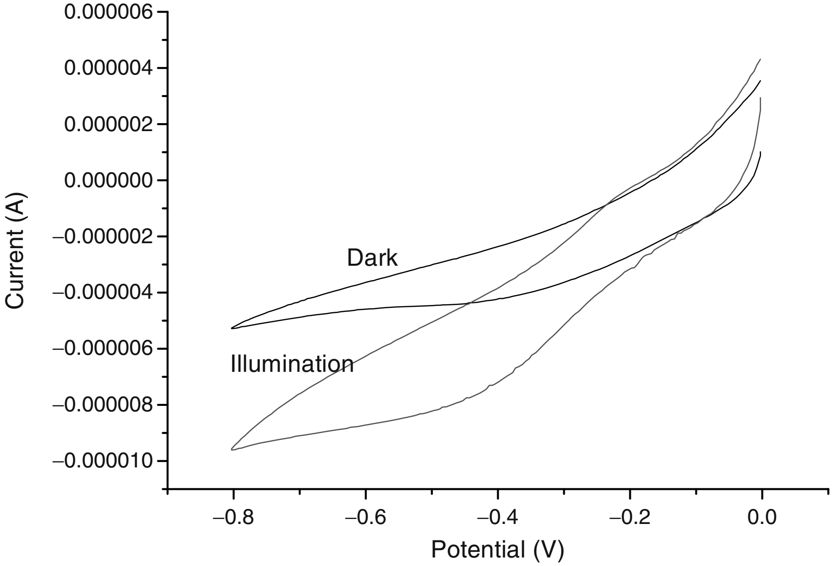

**Fig. 5** Cyclic voltammogram of $Cu_2O$ thin film deposited at −0.4 V on TCO from alkaline lactate solution pH 10 (scan rate 10 mV/s, 0.5 M $K_2SO_4$ electrolyte)

composite film is shifted to a maximum around 400 nm (Fig. 6). The pattern of photo response is similar to that of an n-type semiconductor photo catalyst. It is interesting to note that the maximum IPCE calculated using Equation (1) is 6% at wavelength around 375 nm. The relatively high photo response property of cuprous oxide might be useful for photo catalytic decontamination of water under low light intensity if it is combined with titanium oxide ($TiO_2$).

$$IPCE = \frac{i}{P \times F} \times 100 \tag{1}$$

where i = photocurrent density, F = Faraday constant, P = light intensity (E $s^{-1}$ $cm^{-2}$).

## *3.3 Photo Catalysis and Photoelectrocatalysis with $TiO_2$ Thin Film*

Figure 7 shows the removal of color by photolysis (P), photo catalysis (PC), electrolysis (EC), and photoelectrocatalysis (PEC) using $TiO_2$ electrode as a function of time. No apparent change in methyl orange absorbance was observed by electrolysis alone. Whereas about 10% decrease of the maximum absorption peak of methyl orange was observed under photolysis and 40% decrease was observed under photo catalysis in 24 h reaction time. However, by applying a potential bias of +1.0 V, 100% decrease in

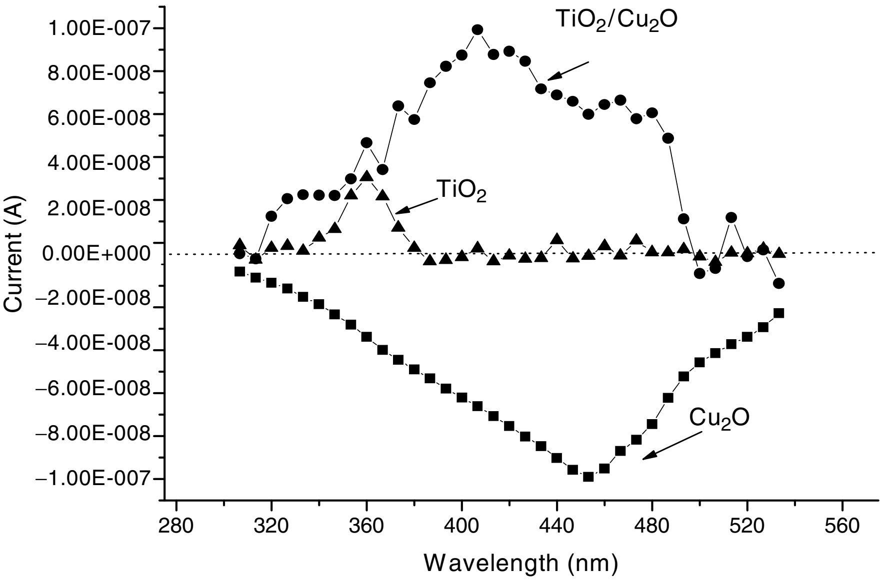

**Fig. 6** Spectral photo response of the electrodes prepared from alkaline lactate solution at pH 10

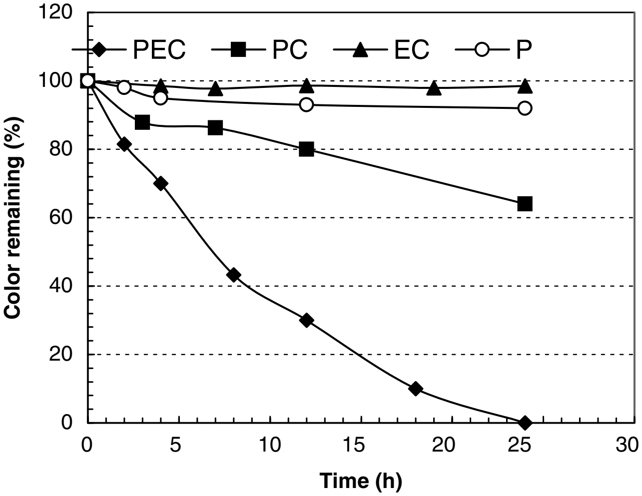

**Fig. 7** Removal of color by photolysis, photo catalysis, electrolysis, and photoelectrocatalysis (+1.0 V) using $TiO_2$ electrode in photoelectrochemical reactor

absorbance was achieved for the same duration of reaction time. The results obtained at pH 6.5 illustrate that under applied potential there is an improvement of the photocatalytic decomposition of the dye. It has been reported that by applying an anodic bias potential higher than the flat-band potential of the semiconductor, the competitive reactions of charge recombination ($e^-/h^+$) can be minimized [17, 28–31]. A potential gradient within the photo catalyst film is provided at potentiostatic conditions to efficiently force the electrons to reach the counter electrode. Therefore photo-generated holes can be trapped in the surface by $H_2O/OH^-$ species to give rise to $OH^\bullet$ radicals, which are essential for promoting the efficient degradation of dyes. It has been reported that the photoelectrocatalytic reaction may depend on applied potential, solution pH, and the type of electrolyte used [30–32].

## 3.4 Effect of pH on Photoelectrocatalytic Degradation Rate

The investigation on the kinetics of methyl orange degradation in aqueous solution under light irradiation was performed and absorbance reduction rate was assumed to follow a pseudo first-order model according to the following Equation (4):

$$\left(\ln \frac{A_t}{A_o}\right) = -Kkt = -k_{app}t \tag{2}$$

where $A_o$ is the initial absorbance, $A_t$ is absorbance at time $t$, $k$ is the reaction rate constant, and $K$ a constant associated with light intensity, adsorption behaviour of methyl orange, and the electric field.

The absorbance had an exponential relationship to reaction time and the apparent first-order rate constant $k_{\mathrm{app}}$ could be calculated from Equation (2). A plot of $\ln(A_t/A_0)$ versus time represents a straight line as shown in Fig. 8, the slope of which upon linear regression equals the apparent first-order rate constant $k_{\mathrm{app}}$, which is a function of light intensity, adsorption behaviour of methyl orange, and the electric field. The degradation rate was also increased either in acidic (pH 2) or alkaline (pH 10) conditions compared to the neutral (pH 6.5) solution. The reaction rate was decreased when the initial concentration of methyl orange increased at a given pH.

The pH is related to the ionization state of the surface as well as to that of reactants, and to the change of flat band potential of the semiconductor electrode. As illustrated in Fig. 9, both the acidic and alkaline conditions favored color removal and almost complete removal of color was realized in electrochemically assisted photocatalytic degradation process at 6h in acidic media. In neutral and alkaline media, the powerful electron-donating dimethylamino group generates a $\pi$-$\pi^*$ transition which lies in the visible region of the spectrum ($\lambda_{\mathrm{max}} = 464\,\mathrm{nm}$) with typical orange color. The molar extinction coefficient of this charge transfer transition is low ($\lambda_{\mathrm{max}}$ [464] = $267\,\mathrm{M}^{-1}\,\mathrm{cm}^{-1}$). The wavelength of maximum absorption shifts to a higher value when the pH is decreased due to protonation of the azo group to form the azonium ion [33]. It is known that pH values can influence the adsorption of dye molecules onto the catalyst surfaces [30, 32, 34]. The flat band potential $E_{\mathrm{fb}}$ is a well-known function of the electrode characteristics and the pH of the solution ($E_{\mathrm{fb}} = E^0_{\mathrm{fb}} + 0.05915$ pH) and follows Nernstian behaviour with a slope of −59 mV. The applied potential is positive to the flat band potential (−0.808 V). Therefore, there is always a potential gradient over the titania film, resulting in an electric field, which keeps photogenerated charges apart.

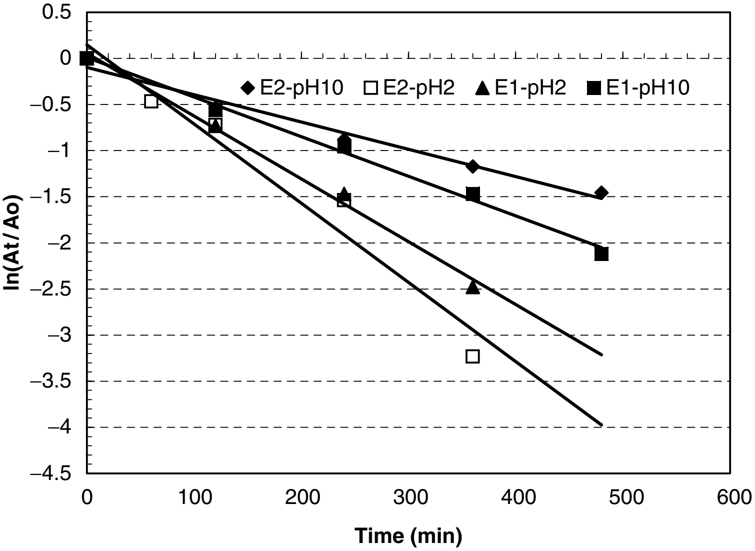

**Fig. 8** Effect of pH on photoelectrocatalytic color removal at bias potential of +1.5 V using $TiO_2$ thin film electrodes

Under alkaline condition, the color removal rate may be affected by an increase in the density of $TiO^-$ groups on the semiconductor electrode surface. Due to the coulombic repulsion, no direct electrostatic interaction between methyl orange and $TiO_2$ particles can occur. However, since the anode is a positively charged electrode, the influence of electric field becomes predominant on the electrode surface. As a consequence, the interaction of the methyl orange with the electrode surface is both potential and pH-dependent. As illustrated in Fig. 9, the apparent rate constant dramatically increases at higher pH values. This might suggest that different mechanisms take place. It is assumed that the electric field due to applied potential control the interaction of methyl orange and $TiO_2$ electrode.

In high alkaline solutions (pH > 10), since hydroxyl radicals are easier to be generated by oxidizing more hydroxide ions available on $TiO_2$ surface according to reactions (3–4), the efficiency of the process is logically enhanced. The minority charge carriers photo generated upon illumination on the photo anode can oxidize the $H_2O/OH^-$ producing $OH^{\bullet}$ radicals that adsorb on the photo electrode surface with the release of $H^+$ ions to the solution.

$$TiO_2 + hv \rightarrow TiO_2\text{–}e^-_{cb} + TiO_2 - h^+_{cb} \tag{3}$$

$$TiO_2 - h^+_{cb} + H_2O_s \rightarrow TiO_2\text{–}OH^{\cdot}_s + H^+ \tag{4}$$

$$TiO_2 - h^+_{cb} + HO^-_s \rightarrow TiO_2\text{–}OH_s \tag{5}$$

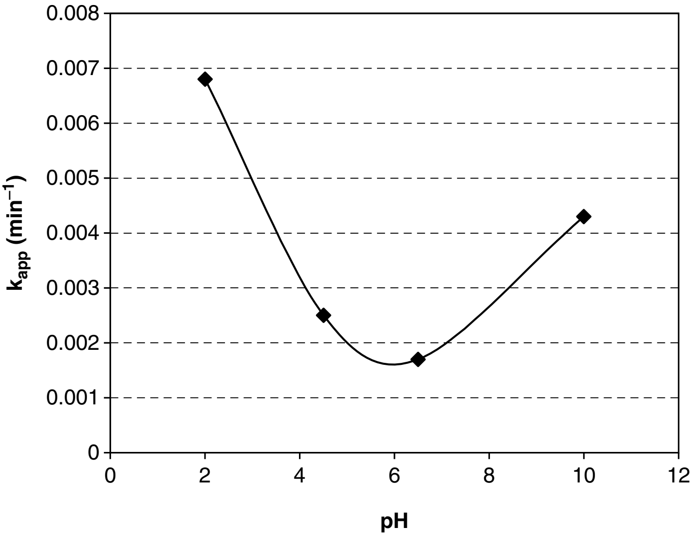

**Fig. 9** Variation of apparent reaction rate constant as a function of pH at bias potential of +1.5 V using $TiO_2$ thin film electrode

On the other hand, the drastic increase in the discoloration rate at lower pH may follow a different mechanism. Methyl orange is an anion in aqueous solution, whose absorption spectrum remains invariant in the pH range 4–14, but changes below pH 4, as expected for protonation of the nitrogen atom of the azo linkage. Whereas the unprotonated compounds is an electron donor, the protonated species has electron-withdrawing character. At the same time, the $TiO_2$ particles are positively charged at low pH values and the semiconductor electrode is also positively charged. The improved photocurrent behavior in the presence of oxygen suggests that the oxygen may pick up the conduction band electron in $TiO_2$ particles, leading to the production of peroxy radical according to the reactions (6–7) (data not shown).

$$O_2 + e^-_{cb} \rightarrow O_2^{\cdot -} \tag{6}$$

$$O_2^{\cdot -} + H^+ \rightarrow {}^{\cdot}OOH \tag{7}$$

Indeed experiments conducted without oxygen supply at low pH indicated lower reaction rate. Peroxide radicals are reported to be responsible for the heterogeneous $TiO_2$ photodecomposition of organic substrates such as dyes [35]. Further, since methyl orange has a sulfuric group in its molecular structure, which is negatively charged, the acidic solution favors adsorption of dye onto the photo catalyst surface, leading to the improvement of the degradation efficiency to some extent. More investigation is required in this regard to elucidate the predominant reaction mechanisms.

Investigation of the influence of the type of electrolyte on the removal of color with 20 mg/L of methyl orange in 0.1 M $K_2SO_4$ and KCl solutions (Fig. 10) showed that there is no significant difference of color removal under the two supporting electrolyte conditions. This indicates that the photo catalytic oxidation reaction of chloride and sulfate or electrochemical oxidation of chloride ion to chlorine at potentials around +1.3 V versus Ag/AgCl is not significant under the experimental conditions used in this study, as shown previously by others [36, 37].

## *3.5 Effect of Applied Potential*

The effect of applied potential on the photoelectrocatalytic degradation rate of methyl orange was investigated by comparing the color removal during oxidation of 20 mg/L dye in 0.1 M $K_2SO_4$ at pH 10 in order to check for the importance of selecting the best potential for this process. Potentials ranged between –0.6 and +2.5 V was applied and the decrease in absorbance at 464 nm was monitored. The results in Fig. 11 show that the apparent rate constant for the removal of color increases progressively with increase in bias potential. On the other hand, the current produced was increased as the applied potential increased (data not shown). This indicates the influence of the applied potential to force the transport of photoelectrons across $TiO_2$ film and also the photo generated electrons are the charge carriers. As anodic potential increased, a large amount of current carrier (photoelectrons) passed through the $TiO_2$ film. Additionally, photogenerated holes were consumed by methyl orange in

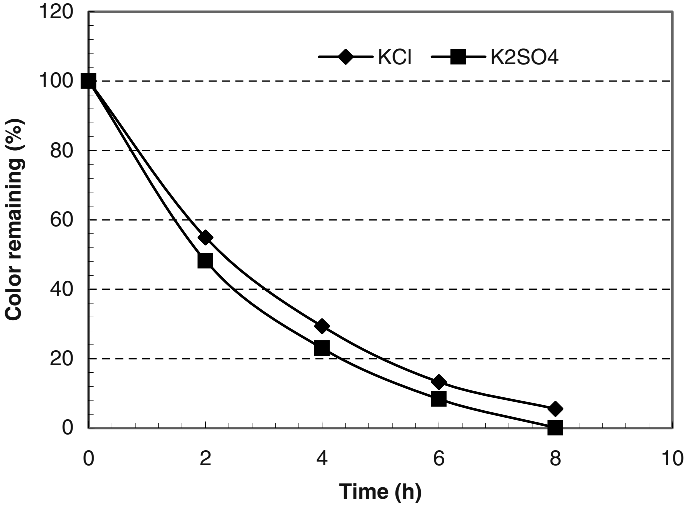

**Fig. 10** Color removal as a function of irradiation time at pH 2 with $TiO_2$ thin film electrodes (E1) at bias potential of 1.5 V in KCl and $K_2SO_4$ supporting electrolytes

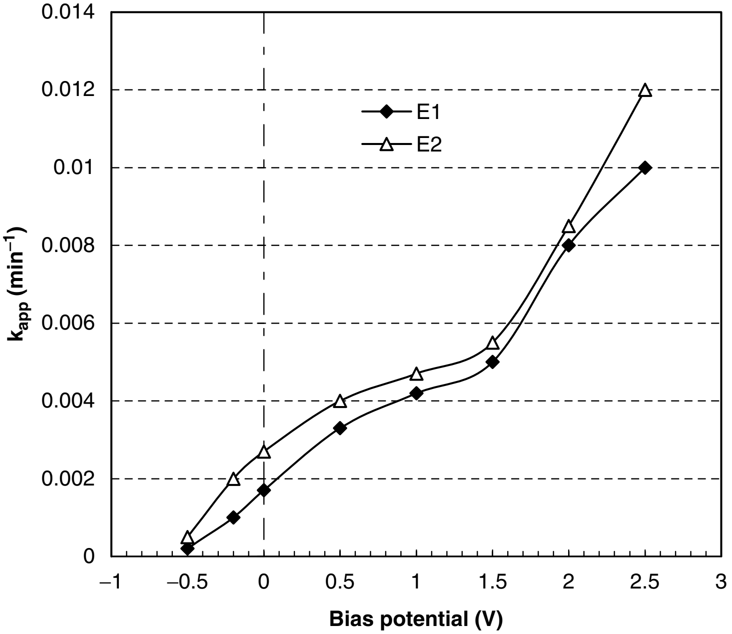

**Fig. 11** Dependence of the apparent reaction rate constant (min$^{-1}$) as function of time at different potential in $K_2SO_4$ at pH 10 using $TiO_2$ thin film electrodes

the solution, which is reflected in the decrease of absorbance. The standard electrode potential values for the couple $OH^{\bullet}$, $H^+/H_2O$ and $O_3$, $2H^+ / O_2$, $H_2O$ are +2.7 and 2.076 V, respectively [37]. The potential applied across the electrodes was 1.5 V in this study and $OH^{\bullet}$ radicals could not be formed by anodic oxidation under the conditions examined. The result shows that color removal was mainly attributed to photocatalytic degradation in the experiments involved.

When the potential exceed 1.5 V, the reaction rate become faster and deviation from linearity was observed. The deviation from linearity at higher potential is associated with the combined effect of the generation of more oxidants at the anode. Overall, the application of a positive potential higher than the flat-band potential on the $TiO_2$ electrode decreases the charge recombination process shown by reaction (8).

$$TiO_2 - h^+_{cb} + TiO_2 - e^-_{cb} \rightarrow \text{Heat} \tag{8}$$

It is interesting to note that the apparent rate constant approach zero as the applied potential approach the flat band potential of $TiO_2$ semiconductor (pure anatase) at pH 10 for the two electrodes. This indicates that charge recombination reaction become predominant if the applied potential is not sufficient for the separation of charge carriers. A slightly higher reaction rate was observed for the electrode made of 100 nm particles (E2).

### 3.6 $TiO_2/Cu_2O$ Composite Electrode System

The apparent rate constant for the removal of color by $TiO_2/Cu_2O$ thin film electrode as a function of bias potential is shown in Fig. 12. Preliminary screening tests (data not shown) indicated that the $Cu_2O$ electrodeposited for 5 min at galvanostatic condition (0.2 mA/cm$^2$) showed better catalytic activity. Good removal efficiency was observed in the potential range −0.6 to −0.2 V *vs.* SCE. This potential range corresponds to the stability range of the $Cu_2O$ [27].

At potential below −0.6 V, formation of reduction to Cu was observed and the electrode surface was gradually changed to black color. The color removal continued at reduced rate, possibly due to the catalytic activity of $TiO_2$/Cu system. On the other hand, the reduction in catalytic activity was more pronounced at positive bias potential. This indicates that only $Cu_2O$ has strong contribution to the removal of color and further oxidation to other copper oxide species may inhibit the catalytic activity of $TiO_2$. It is interesting to note that apparent rate constant obtained at −0.4 V for the composite thin film (Fig. 12) is comparable to that of pure $TiO_2$ film at bias potential of +1.5 V.

The enhanced catalytic effect by $Cu_2O$ at this low potential value is possibly due to more efficient electron and hole separation in the composite system. The potential gradient at the interface promotes the electrons and holes to flow in opposite directions, and the photo generated holes migrate towards the interface while the electrons migrate towards $TiO_2$ and then to TCO, making the behavior of the composite film analogous to that of an n-type semiconductor as shown schematically in Fig. 12. It can be concluded that the composite semiconductor electrode may have

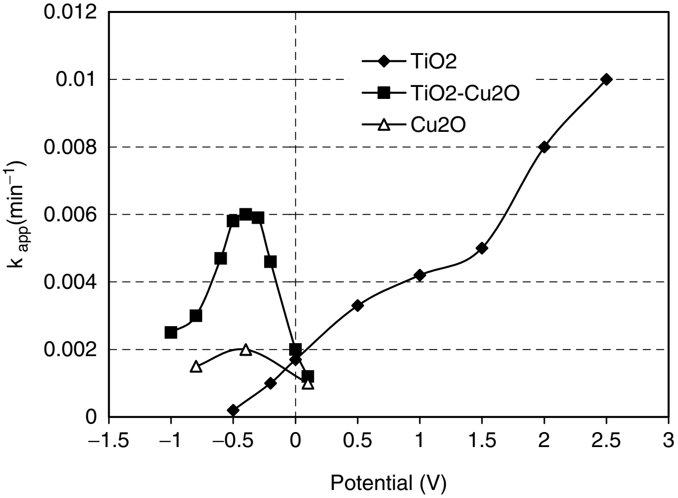

**Fig. 12** Dependence of the apparent reaction rate constant (min$^{-1}$) as function of time at different potential in $K_2SO_4$ at pH 10 using $Cu_2O$, $TiO_2$, and $TiO_2/Cu_2O$ composite thin-film electrodes

better harvesting efficiency of light due to observed shift in absorption spectrum as compared to that of pure $TiO_2$.

$Cu_2O$ in the composite thin films have a beneficial role in improving charge separation and may also extend the light absorption spectrum of $TiO_2$.

## 4 Conclusions

The p-type semiconductor $Cu_2O$ electrode prepared from the cupric lactate solution under alkaline condition showed a stable photocurrent over longer time range. The photo response was not changed after repeated use of the electrode. The rate of removal of color by $TiO_2$ thin film electrode was enhanced when potential bias of 1.5 V was applied. The $TiO_2/Cu_2O$ composite thin film electrode showed an n-type semiconductor photocurrent characteristic. When the $TiO_2/Cu_2O$ thin film electrode was used, the color removal rate reach maximum, at potential bias of –0.4 V. Further increase or decrease of bias potential caused decreased reaction rate. It is considered that the photo-generated holes migrate towards the interface while the electrons migrate towards $TiO_2$ and then to the back contact (TCO), making the behavior of the composite film analogous to that of an n-type semiconductor. $Cu_2O$ in the composite thin films have a beneficial role in improving charge separation and may also extend the light absorption spectrum of $TiO_2$ to the visible region of the electromagnetic spectrum. In all cases, the kinetics of the photocatalytic oxidation of methyl orange followed a pseudo first order model and the apparent rate constant may depend on several factors such as, the nature and concentration of the organic compound, radiant flux, the solution pH and the presence of other organic substances.

**Acknowledgements** This research was financially supported by the Organization for the Prohibition of Chemical Weapons (OPCW), The Hague, The Netherlands, and the Netherlands Government.

## References

1. Serpone, N.; Pelizzetti, E. Photocatalysis Fundamentals and Application. 1st ed., Wiley, New York, **1989**.
2. Hagfeldt, A.; Gratzel, M. *Chem. Rev.* **1995**, 95, 49–68.
3. Karkmaz, M.; Puzenat, E.; Guillard, C.; Herrmann, J.M. *Appl. Catal. B: Environ.* **2004**, 51, 183–194.
4. Chen, C.; Lu, C.;Chung, Y. *J. Photochem. Photobiol. A: Chem.* **2006**, 181, 120–125.
5. Fox, M.A.; Dulay, M. T. *Chem. Rev.* **1993**, 93, 341–357.
6. Fujishima, A.; Rao, T.N.; Tryk, D.A. *J. Photochem. Photobiol. C: Photochem.* **2000**, 1, 1–21.
7. Cordoba, G.; Viniegra, M.; Fierro, J.L.G.; Padilla, J.; Arroyo, R. *J. Solid State Chem.* **1998**, 138, 1–6.
8. Fujitsu, S.; Hamada, T. *J. Am. Ceram. Soc.* **1994**, 77(12), 3281–3283.
9. Wilke, K.; Breuer, H.D. *J. Photochem. Photobiol. A: Chem.* **1999**, 121, 49–53.

10. Spanhel, L.;Weller, H.; Henglein, A. *J. Am. Chem. Soc.* **1987**, 109(22), 6632–6635.
11. Zhou, H.S.; Honma, I.; Komiyama, H.; Haus, J.W. *J. Phys. Chem.* **1993**, 97(4), 895–901.
12. Hotchandani, S.; Kamat, P.V. *J. Phys. Chem.* **1992**, 96(16), 6834–6839.
13. Bedja, I.; Kamat, P.V. *J. Phys. Chem.* **1995**, 99(22), 9182–9188.
14. Tristao, J.C.; Magalhaes, F.; Corio, P.; Sansiviero, C. *J. Photochem. Photobiol. A: Chem.* **2006**, 181, 152–157.
15. Wang, W.; Silva, C.G.; Faria J.L. *Appl. Catal. B: Environ.* **2006**, in press.
16. Xiaodan, Y.; Qingyin, W.; Shicheng, J.; Yihang, G. *Mater. Charact.* **2006**, in press.
17. Hepel, M.; Hazelton, S. *Electrochim. Acta* **2005**, 50, 5278–5291.
18. Grozdanov, I. *Mater. Lett.* **1994**, 19, 281–285.
19. Mizuno, K.; Izaki, M.; Murase, K.; Shinagawa, T.; Chigane, M.; Inaba, M.; Akimasa, T.; Awakura, Y. *J. Electrochem. Soc.* **2005**, 152(4), 179–182.
20. Khan, K.A. *Appl. Energ.* **2000**, 65, 59–66.
21. Hara, M.; Kondo, T.; Komoda, M.; Ikeda, S.; Kondo, J.N.; Domen, K., Shinohara, K.; Tanaka, A. *Chem. Commun.* **1998**, 4, 357–358.
22. Vigil, E.; Gonza'lez, B.; Zumeta, I.; Domingo, C.; Dome'nech, X.; Ayllo'n, J.A. *Thin Solid Films* **2005**, 489, 50–55.
23. Golden, T.D.; Shumsky, M.G.; Zhou, Y.; VanderWerf, R.A.; Van Leeuwen, R.A.; Switzer, J.A. *Chem. Mater.* **1996**, 8, 2499–2504.
24. Jongh, P.E.; Vanmaekelbergh, D.; Kelly, J.J. *J. Electrochem. Soc.* **2000**, 147(2), 486–489.
25. Bohannan, E.W.; Shumsky, M.G.; Switzer, J.A. *Chem. Mater.* **1999**, 11, 2289–2291.
26. Mahalingam, T.; Chitra, J.S.P.; Rajendran, S.; Jayachandran, M.; Chockalingam, M.J. *J. Cryst. Growth* **2000**, 216, 304–310.
27. Pourbaix, M. Atlas of Electrochemical Equilibria in Aqueous Solutions, 2nd ed., Pergamon Press, New York, **1966**.
28. Jorge, M.A.; Sene, J.J.; Florentino, A.O. *J. Photochem. Photobiol. A: Chem.* **2005**, 174, 71–75.
29. Zainal, Z.; Lee, C.Y. *J. Sol-Gel Sci. Tech.* **2006**, 37, 19–25.
30. Li, G.; Qu, J.; Zhang, X.; Ge, *J. J. Mol. Catal. A: Chem.* **2006**, 259, 238–244.
31. Zanoni, M.V.B.; Sene, J.J.; Anderson, M.A. *J. Photochem. Photobiol. A: Chem.* **2003**, 157, 55–63.
32. Candal, R.J.; Zeltner, W.A.; Anderson, M.A. *Environ. Sci. Technol.* **2000**, 34, 3443–3451.
33. Oakes, J.; Gratton, P. *J. Chem. Soc. Perk. Trans.* **1998**, 2, 2563–2568.
34. Galindo, C.; Jacques, P.; Kalt, A. *J. Photochem. Photobiol. A: Chem.* **2000**, 130, 35–47.
35. Hoffmann, M.R.; Martin, S.T.; Choi, W.; Bahnemann, D.W. *Chem. Rev.* **1995**, 95, 69–96.
36. Mills, A; Hunte, S. *J. Photochem. Photobiol. A: Chem.* **1997**, 108, 1–35.
37. Konstantinou, I.K.; Albanis, T.A. *Appl. Catal. B: Environ.* **2004**, 49, 1–14.